Review article

Nancy M. Haegel*

Integrating electron and near-field optics: dual vision for the nanoworld

Abstract: The integration of near-field scanning optical microscopy (NSOM) with the imaging and localized excitation capabilities of electrons in a scanning electron microscope (SEM) offers new capabilities for the observation of highly resolved transport phenomena in the areas of electronic and optical materials characterization, semiconductor nanodevices, plasmonics and integrated nanophotonics. While combined capabilities for atomic force microscopy (AFM) and SEM are of obvious interest to provide localized surface topography in concert with the ease and large spatial dynamic range of SEM and dual beam imaging (e.g., *in-situ* AFM following focused ion beam modification), integration with near-field optical imaging capability can also provide access to localized transport phenomena beyond the reach of far-field systems. In particular, the flexibility that is achieved with the capability for independent, high resolution placement of an electron source, providing localized excitation in the form of free carriers, photons or plasmons, with scanning of the optical collecting tip allows for unique types of "dual-probe" experiments that directly image energy transfer. We review integrated near-field and electron optics systems to date, highlight applications in a variety of fields and suggest future directions.

Keywords: near-field scanning optical microscope; scanning electron microscope; integrated; cathodoluminescence; transport imaging; diffusion; energy transport.

***Corresponding author: Nancy M. Haegel,** Naval Postgraduate School – Physics, 833 Dyer Rd, Monterey, CA 93943, USA, Phone: +831 656 3954, e-mail: nmhaegel@nps.edu

Edited by Aaron Lewis

1 Introduction

Two approaches have been pursued historically to improve optical resolution in order to observe and characterize smaller and smaller phenomena: 1) decrease the wavelength of the imaging radiation, as in electron microscopy, or 2) circumvent the far-field diffraction limit through the use of near-field imaging. Edward Hutchison Synge introduced the concept of near-field imaging in 1928 [1]. It has been reported that in the same year, Leo Szilard suggested the basic concept of a scanning electron microscope in conversations with colleagues; Szilard filed a German patent application for such a device on July 4th, 1931 [2].

Ernst Ruska is credited with building the first electron microscope in 1933. Cambridge Instruments and JEOL began making commercial instruments widely available in 1965 and Ruska was awarded a much delayed Nobel Prize in Physics in 1986. For near-field imaging, the time from conception to demonstration was longer. Ash and Nicholls published the first experimental demonstration in 1972 using millimeter waves [3], with work at visible wavelengths appearing a decade later. The first commercial NSOM, the Topometrix Aurora, went on the market in 1994. In 2004 Nanonics Imaging Ltd. introduced a commercial AFM/NSOM system allowing for optical access to the collecting tip and, also importantly, the option for independent scanning of the NSOM probe, as well as the sample. While the scanning tunneling microscope had a very short interim between the first demonstration of its new imaging capability and a Nobel Prize for its inventors (1981–1986, sharing the Nobel Prize in Physics with Ernst Ruska), a duration of 53 years similar to that experienced by Ruska might project a Nobel Prize related to scanning probe optical imaging for sometime in the period from 2025 to 2035.

Eighty-five years after the SEM and NSOM were independently envisioned, we now see the integration of these two approaches. An increasingly localized electron beam probe can be combined with near-field optical collection to reach new resolution limits and image phenomena associated with the generation of light and the transport of energy in nanostructured materials and devices.

2 Early systems

The earliest integrations of SEM and AFM/SPM (scanning probe microscopy) were focused on providing high

© 2014 Science Wise Publishing & De Gruyter

Brought to you by | Arthur Lakes Library
Authenticated | 10.248.254.158
Download Date | 8/24/14 1:24 PM

resolution surface topography associated with AFM with the wide dynamic imaging range of SEM. In introducing a “universal SPM-based hybrid system” for incorporation into an SEM chamber in 2003, Joachimsthaler et al. [4] review some of the earliest systems and point out the challenges of integration while maintaining optimum capability for both types of imaging. This is particularly true with respect to the working distance of the SEM, which plays a key role in obtaining optimum SEM imaging at high magnification. The growing importance of focused ion beam for *in-situ* modification of materials and devices may well drive further AFM/SEM commercial development of integrated systems and will be discussed briefly at the end of the review.

Integration for the primary purpose of collecting luminescence generated by an electron beam with a near-field probe [near-field cathodoluminescence (CL)] was first presented in 1998 [5, 6]. Troyon et al. used a home-built scanning force microscope (SFM), with a laser-based cantilever deflection system and a four-quadrant photodetector. The SFM was mounted inside the chamber of a Gemini 982 field emission Leo SEM (LEO, Oberkochen, Germany). An optical multimode fiber was placed above a Si_3N_4 pyramidal tip to locally diffract the light and cause the signal to propagate to the collecting fiber. High resolution imaging of Er-doped CaF_2 was demonstrated with a reported resolution on the order of 100 nm [5].

Cramer et al. designed a system with interchangeable probe mounts for STM, SFM or NSOM, with the probe and sample tilted at 60° with respect to the electron beam [6]. The SPM was based on a prototype of the TopoMetrix Observer SPM integrated with a CamScan S2. Their NSOM probe was a metal-coated optical fiber on a piezoelectric tuning fork. In order to increase detection sensitivity, a beam-blanker was used to modulate the electron beam excitation, allowing for lock-in detection of the optical signal. They observed CL emission in bulk yttrium aluminum garnet (YAG) with a reported resolution, based on intensity variations, of 50 nm.

Schematics from these two systems are presented in Figure 1. Electron beam access to the point of contact of the optical probe was achieved by tilting of the sample relative to the incident electron beam. Both systems allowed for scanning of the electron probe in standard SEM operation and for scanning of the sample, but the position of the collecting probe tip was fixed. While this works fine for high resolution CL imaging, it limits some other capabilities that are of interest for integrated electron beam/near-field systems.

Several challenges were quickly apparent in the early work. First, electrical charging associated with both the specimen and the probe tip needed to be eliminated or minimized. In the absence of attention to appropriate grounding and coating, significant local drift and even tip deformation were observed. Second, limited optical collection as determined by the throughput of NSOM optical fiber tips or the efficiency of scattering and absorption in the presence of another type of dielectric tip required dealing with the reality of small signals. Finally, questions about the role of background luminescence associated with far-field effects, whether due to the extent of the generation volume from the incident electron beam, or local transport of the generated free carriers or photons, needed to be understood.

The combination of an NSOM with an SEM effectively provides an alternate approach to the dual-probe capability that is increasingly desired in NSOM and other SPM systems [7, 8]. Multi-probe systems for highly localized electrical measurements have been operated inside of SEMs in order to directly image probe-to-probe distances that could not be optically resolved. In the case of NSOM integrated into an SEM, the electron beam can be utilized both for imaging the localization of the collecting probe (e.g., somewhere on a particular nanostructure) and simultaneously as a localized probe/generation source when operated in spot or line mode. While it can be challenging in dual-probe NSOM systems to position and scan the two probes with nanometer proximity, the SEM makes it easy to position the electron beam anywhere in relationship to an NSOM probe on a sample.

There are multiple approaches then for imaging and data acquisition, based on three possible scanning options: A) the sample, with electron beam and collecting probe fixed in relative proximity to each other; B) the electron beam, with the collecting probe fixed at a spot on the sample; and C) the collecting probe, with electron beam excitation fixed at a spot on the sample. A system that allows for all three scanning modes provides the highest flexibility for various types of experiments and, in particular, for the high spatial mapping of excitations generated by the electron beam that result in carrier transport, waveguiding or plasmon-assisted CL. Figure 2 summarizes the range of options.

In NSOM systems with excitation via laser sources, it is common to refer to *illumination mode* (**I** – near-field excitation through the NSOM tip, far-field detection via an optical microscope), *collection mode* (**C** – near-field collection via the NSOM tip, far-field excitation with a laser through the objective of an optical microscope), *combined I-C* mode (**I/C** - excitation and collection via the same NSOM probe tip) and *dual-probe* (independent excitation **I** and collection **C** NSOM probes). Using the electron beam for highly localized excitation with a near-field imaging probe potentially creates a dual-probe experiment using

Brought to you by | Arthur Lakes Library
Authenticated | 10.248.254.158
Download Date | 8/24/14 1:24 PM

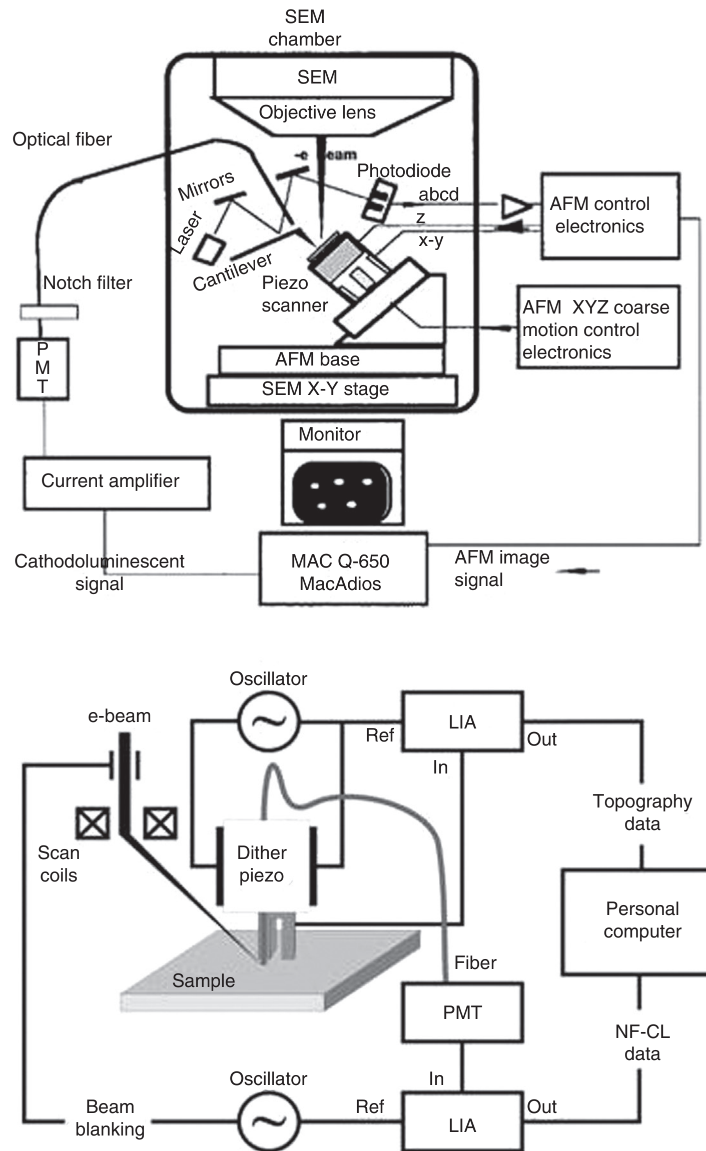

Figure 1 Schematic diagram of earliest systems to integrate near-field optical scanning microscopy into scanning electron microscopes. Upper: System of Troyon et al. [5]. Lower: System of Cramer et al. [6]. Both systems were used to demonstrate imaging of CL emission in the near-field by scanning the sample with the electron beam fixed adjacent to the collecting probe. Figures reprinted with permission from Ref. [5] and Ref. [6]. Copyright 1998 AIP Publishing LLC.

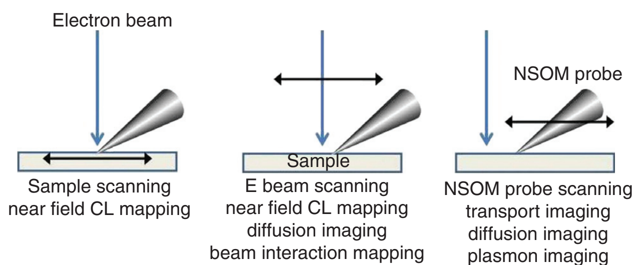

Figure 2 Schematic illustrating scanning options and associated experiments.

only one actual NSOM probe. The exact nature and extent of the excitation in this case, however, depend strongly on the particular electron beam/sample interaction.

In the remainder of the review, we highlight work performed in integrated SEM/NSOM instruments in the areas of near-field CL and transport imaging and conclude with a discussion of future directions for research and development. For broader recent reviews of NSOM and scanning probe microscopies for high resolution spectroscopy, readers are referred to Refs. [9] and [10].

Brought to you by | Arthur Lakes Library
Authenticated | 10.248.254.158
Download Date | 8/24/14 1:24 PM

3 Near-field cathodoluminescence

Conventional cathodoluminescence uses an electron beam to excite luminescence which is then collected in the far-field, generally with a parabolic mirror that directs the photons to a photodiode, photomultiplier or CCD array. CL has played an important role in the characterization of semiconductors, minerals and other fluorescent materials [11]. The electron beam is generally scanned over the sample to create a luminescent map of the material, assuming that the light emitted can be mapped back to the point of excitation. The resolution of conventional CL is limited by a complex combination of the generation volume of the electron beam in the particular sample and energy transport from the source in the form of either excess carrier diffusion, waveguiding or photon recycling. In photon recycling, photons that are locally generated by recombination in the generation region can propagate in the material and then be reabsorbed and re-emitted.

Near-field cathodoluminescence was introduced with the goal of improving the spatial resolution by restricting the measured luminescent area via the use of the near-field collecting tip. With the collecting probe fixed at a spot immediately adjacent to the point of electron beam excitation, the sample can be scanned underneath to produce a map of the spatial variations of the luminescence where the region from which the light is collected can be more restricted than in traditional far-field CL. Two different collecting approaches were initially demonstrated: 1) a high resolution SPM dielectric probe converting the local field into propagating waves which were then collected in the far-field by a fiber suspended about 50 µm above the sample [5] and 2) small diameter aperture fiber tips directly in SPM feedback just nanometers above the sample surface [6].

Since the primary motivation is generally presented as improved resolution, it is important to understand the relevant limiting factors, placing them in context of the near-field photoluminescence work that is more familiar to most users. One significant factor is whether the source of the potential luminescence is extended or geometrically isolated. An example of an extended source would be any bulk material, thin film or even micron scale particles that are significantly larger than the excitation dimensions. Geometrically confined and isolated luminescent sources might include quantum wells, quantum dots, or single molecules. There are multiple length scales in the problem that need to be identified. These include:

1. the dimensions of the luminescent structure (extended or confined in x and/or y and/or z), $\mathbf{X}(x, y, z)$
2. the dimension of the collecting tip $\boldsymbol{\varphi}$
3. in many materials, the diffusion length for free carriers created by the excitation beam, or other relevant energy transfer mechanisms, $L_{\mathrm{d}}=\sqrt{\frac{kT}{e}\mu\tau}$
4. the excitation region/volume. For laser excitation, this is effectively the area of illumination, either in the far-field or via the NSOM probe, with a characteristic depth given by α^{-1}, where α is the absorption coefficient for the wavelength of the incident light.

It is helpful to differentiate here between resolution, as typically understood, and the volume of sampled material that contributes to a luminescent signal derived from a particular spot or region. The focus here is on materials in which luminescence is being generated in the material by the incident electron beam (as opposed, for example, to imaging of reflected light from small structures or apertureless NSOM fluorescence of particles on a surface excited by evanescent waves in a supporting substrate [12]). Although the light may be obtained from a near-field measurement in a highly restricted region (e.g., the area immediately under the near-field probe), it is possible that light generated at more remote locations in the sample is coupled into that localized measurement. This is particularly true in the case of semiconductors, which have a relatively high index of refraction and therefore a significant amount of internally reflected luminescence that can be converted to propagating waves by the NSOM measurement. Correspondingly, carriers generated in a highly localized fashion can diffuse and recombine at more remote locations, extending the sampled volume observed in the far-field even with localized near-field excitation [13].

When the luminescent structure is geometrically confined, however, these effects become less critical, either because the surrounding material does not luminesce, or its luminescence occurs at a different wavelength. In this case, the sampled region just depends on the structure size and spatial imaging is determined by convolution of the structure and the collecting or exciting probe [14]. The range of possibilities is summarized in Table 1 for the NSOM photoluminescence case.

Electron beam excitation in the SEM combined with collection via a near-field probe is most appropriately compared to the collection mode in optical NSOM if the region of excitation, though still highly localized, is broadened beyond the dimensions of the collecting probe by either the excitation volume of the electrons or subsequent energy transfer via carrier diffusion. The generation volume is determined by the size of the electron beam, its energy and associated penetration depth in a given

Brought to you by | Arthur Lakes Library
Authenticated | 10.248.254.158
Download Date | 8/24/14 1:24 PM

Table 1 Factors determining the optically sampled volume for different types of illumination and collection in near-field systems, for both extended and localized sources.

Luminescent source	I Near-field illumination, far-field collection	C Near-field collection, far-field illumination	IC Coupled near-field illumination, near-field collection
Extended X(x, y, z) >> φ	Convolution of φ, L_d	Convolution of φ and evanescent signal from region dependent on L_d, α^{-1}	Convolution of φ and L_d and resulting evanescent signal from region dependent on Ld and α^{-1}; Smallest sampled volume but highly limited signal
Localized X(x, y, z) ~ φ	Convolution of X, φ	Convolution of X, φ	Convolution of X, φ

X represents the sample size/geometry and ϕ is the dimension of the NSOM probe aperture. L_d is the carrier diffusion length and α is the absorption coefficient for the incident illumination.

material (the equivalent of α^{-1} for optical excitation). For extended luminescence, then, the collection of light from the probe area, as discussed, includes both direct emission from the region immediately under the probe, as well as potential contribution from the coupling of the evanescent waves from this larger excited region.

This “background” contribution has been identified and modeled by Pastre et al. [15, 16]. They investigated the role of the surface recombination and the effect of variation of the absorption coefficient/depth of electron beam penetration. However, as they point out, and as the images obtained in [5, 6] and [17] indicate, the resolution that can be obtained from near-field CL even on extended sources is still a significant improvement over conventional CL and, in many cases, over near-field collection mode photoluminescence. This is because of the ability to highly localize the generation region and the overall improvement when this localized generation is convoluted with the energy transport and collection geometry. Use of low energy electrons can minimize the generation region further, though often with corresponding loss in signal intensity.

For geometrically isolated sources, resolution can be obtained that is limited by a convolution of the dimension of the near-field probe and the luminescent source. For this type of sample, the ability of the electron beam to excite very small regions can be fully utilized, without concern for bulk energy transport. This capability is utilized in transmission electron microscopy to generate very high resolution CL images [18]. This will be discussed further in the concluding section.

An additional concern is the effect of topography on the efficiency of the near-field collection. Nogales et al. demonstrate the ability of near-field CL to image defects that are not seen in conventional CL [19], but also observed the challenge in interpreting topography effects superimposed on the near-field CL image because of the extremely high sensitivity of collection to the probe-specimen distance. Detailed quantitative image analysis that correlates topography changes to NSOM intensity changes, coupled to the transport imaging experiments that will be discussed in the next section, could be helpful in this regard for further isolating material luminescence variations.

Examples of near-field CL imaging include work on bulk YAG, Er doped CaF_2, GaAsP, GaN, AlGaN/GaN and MgO [5–6, 17, 19]. Figure 3 shows an example from near-field CL on a “hillock” structure in GaN, allowing for observation of CL contrast within a 200 nm thick defect structure that is not observed in standard CL.

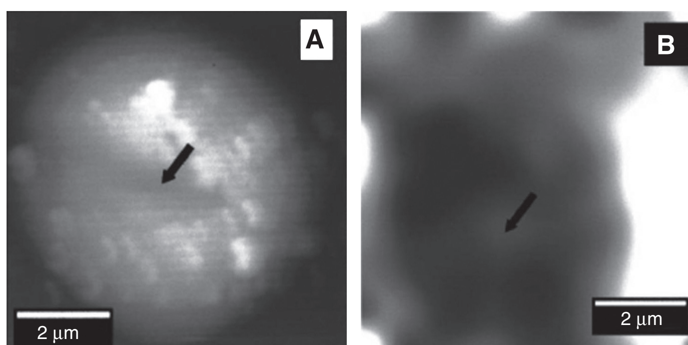

Figure 3 Topography (left) and panchromatic near-field CL image (right) from a GaN structure. Figure reprinted with permission from Ref. [19]. Copyright 2002 AIP Publishing LLC.

Brought to you by | Arthur Lakes Library
Authenticated | 10.248.254.158
Download Date | 8/24/14 1:24 PM

The near-field CL work to date using optical fiber probes has been accomplished with NSOM probe diameters that are significantly larger than those used to achieve the highest reported resolutions in other types of optical studies. Classical diffraction theory shows that the throughput for a sub-wavelength aperture varies as $(d/\lambda)^4$ [20]. This strong dependence on diameter has limited the aperture sizes used to date in near-field CL. As the fiber is tapered to its final aperture, there is also a cut-off diameter for single mode transmission, given by $d \sim 0.6\lambda/n$, where n is the index of refraction [9].

The metal coatings on the fiber play an important role at this point in reducing optical loss below the cut-off diameter. Aluminum is the most common metal coating, since it has the smallest skin depth for visible light, but Au and Cr are also used. Various attempts have been made to increase optical throughput for small diameter apertures, including optimizing the nature of the taper geometry and controlling the final aperture using focused ion beam milling of evaporated metal films [21]. This 2011 work demonstrated a factor of 100× improvement for transmission through a 100 nm diameter aperture, leading to a throughput of 10^{-3}, compared to 10^{-5}. Dissemination of these state-of-the-art approaches throughout the NSOM community will open the resolution/intensity limitation for near-field CL and other experiments.

Growing availability of commercial systems designed to be integrated into SEMs without loss of SEM imaging capability will also play a significant role in expanding the use of near-field CL. In addition, detailed studies of signal intensity and spatial variation comparing contact, tapping, and far-field modes of collection would further clarify issues of limiting resolution and information volume. The trajectory of smaller and smaller devices of interest, which magnifies the importance of spatial material variations at the same small length scales, coupled with the growing requirement for electron beam imaging to observe and manipulate these structures, suggests that near-field CL will also grow in importance and impact as the capability becomes more widespread and more fully understood.

4 Transport imaging

Transport imaging, as we use the term here, combines scanning electron microscopy (SEM) and optical microscopy to "see" electronic transport via imaging of non-equilibrium carrier recombination. Spatially resolved imaging of the resulting luminescence allows observation of the motion of that charge, acquiring steady-state images of the light emitted as some fraction of carriers recombine along their path of travel. While a number of related spatially-resolved experiments have utilized a laser source for generation of charge and collected light in the far-field, (see, for example, Refs. [22–25]), the high degree of localization and the ease of spatial control of the electron beam in the SEM for carrier generation, combined with the near-field mapping of the resulting luminescence pattern, makes this a powerful approach for the study of transport in very small structures and in a wide range of luminescent materials, independent of bandgap.

The approach is related to, but distinct from cathodoluminescence in that it maintains the spatial information of the recombination light, which is lost in traditional scanning photoluminescence or cathodoluminescence. In those techniques, including the near-field CL discussed in the previous section, spatial resolution comes from moving either the source of excitation or the sample. In transport imaging, the source of excitation is fixed and spatial information comes from the distribution of the associated recombination. It is, in essence, a steady-state spatially resolved form of the famous Haynes-Shockley experiment [26], but one with very high spatial resolution that can be performed anywhere on the sample, independent of electrical contact, to observe carrier motion.

Transport imaging in the SEM in thin films and bulk materials has been used to study minority carrier drift in heavily doped materials, anisotropy of minority carrier mobility in solar cell materials, diffusion length variations associated with dislocation networks in mismatched semiconductors and spatial non-uniformities in bulk materials for nuclear radiation detectors [27–31]. In measuring characteristic transport distances, far-field spatial imaging of the luminescent distribution is sufficient (and provides much higher collection efficiency) when the lengths are large. However, for small diffusion lengths and for very small individual structures, the diffraction limitations on the far-field imaging require the use of near-field luminescence mapping.

In 2005, Haegel et al. integrated a Nanonics Multiview 2000 AFM/NSOM (Nanonics Imaging, Ltd., Jerusalem, Israel) into a JEOL 840 SEM (JEOL, Tokyo, Japan) [32]. This AFM/NSOM architecture provides direct optical axis access to the sample for electron beam imaging as well as charge carrier generation. Cantilevered fiber probes are used simultaneously as AFM topography probes and near-field collection tips, with apertures ranging from ~100 to 500 nm. Although the smallest size is desirable for maximum resolution, the d^4 dependence on aperture diameter means a reduction of a factor of 625 in moving from a 500 to a 100 nm tip, without including the effect of lower sampled volume. The minimum aperture that can be used in practice depends greatly on the luminescence of the particular sample.

Brought to you by | Arthur Lakes Library
Authenticated | 10.248.254.158
Download Date | 8/24/14 1:24 PM

The Multiview 2000 allows for independent scanning of the probe, as well as the sample. At the time of system integration, this was the first commercially available system allowing for independent probe scanning that could be integrated in an SEM. This capability is critical for transport imaging because it allows the electron beam to be fixed at any particular point for carrier generation, while the collecting tip is scanned to image carrier transport from that single point of interest. Near-field CL can be performed with sample scanning, but then localized transport can be studied to fully investigate the intensity variations by measuring the diffusion length and associated carrier lifetime, at any point within a specific structure such as a nanowire.

More recently, the system has been integrated with an FEI Inspect 50 SEM (FEI Hillsboro, OR, USA) [33]. Figure 4 summarizes the concept of the integrated system and Figure 5 shows a photograph of the AFM/NSOM inside the SEM chamber. A minimum working distance of ~10 mm can be obtained by limiting large scale stage translation and allowing the pole piece to approach the sample within the open region in the top plate of the NSOM instrument.

Figure 6 shows an SEM image of an NSOM probe above a sample with a mixture of ZnO nanowires and nanobelts. The light collected via the NSOM tip exits through a vacuum fiber feedthrough and is detected by an external photodiode or photomultiplier tube, depending on the desired wavelength detection range. Positioning of the tip with respect to the nanostructure of interest is accomplished via the "inertial motion" feature of the Multiview 2000, which allows for movement of the sample relative to the probe tip via pulsed motion for a maximum travel of ~6 mm. Using this capability, a large number of the individual structures seen in Figure 6 could be measured without the need to externally reposition the sample or the NSOM tip. Then finer spatial control of the tip is obtained via positioning through the piezo controls. The maximum scan range is ~70×70 μm.

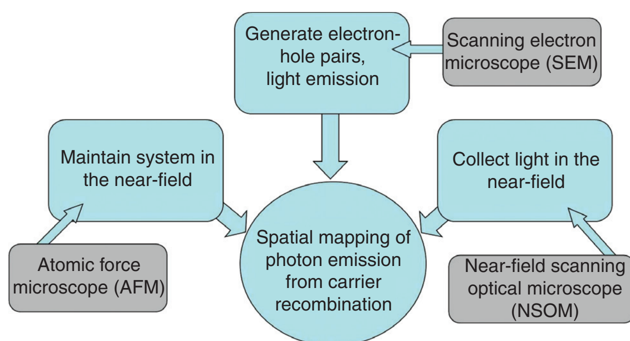

Figure 4 Transport imaging via integrated operation of three scanning microscope capabilities.

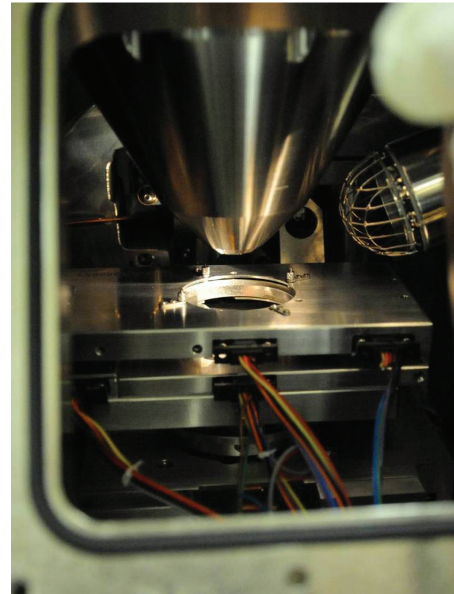

Figure 5 Photograph of AFM/NSOM inside SEM chamber. Electron beam is incident perpendicular to the sample.

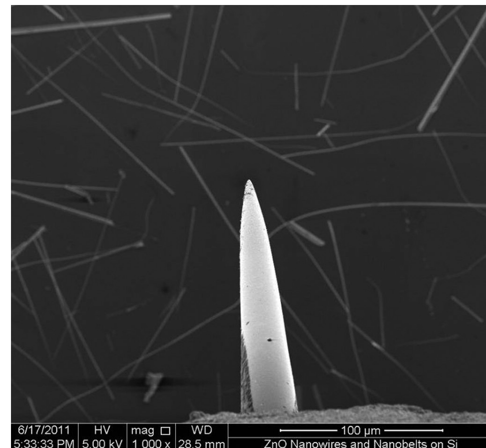

Figure 6 SEM image of NSOM collecting probe in a region of multiple ZnO nanowires.

A variety of transport phenomena can be observed and quantified, including carrier diffusion, carrier drift and photon waveguiding. Figure 7 shows an NSOM image of a luminescence profile from excess carrier diffusion and recombination in a GaAs thin film double heterostructure. The luminescence distribution reflects the minority carrier diffusion length in the material and the associated mobility lifetime (μτ) product:

$$L_d = \sqrt{\frac{kT}{e}\mu\tau}$$

Brought to you by | Arthur Lakes Library
Authenticated | 10.248.254.158
Download Date | 8/24/14 1:24 PM

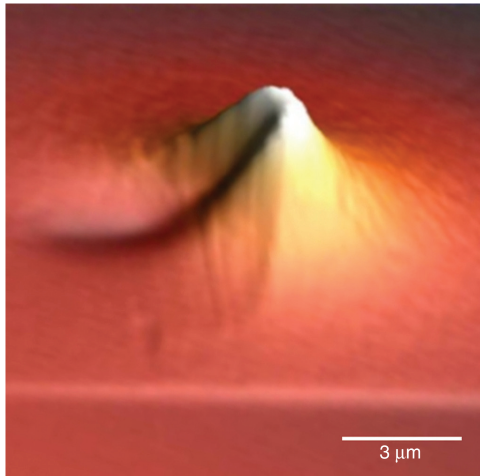

Figure 7 NSOM image showing distribution of carrier recombination in a GaAs double heterostructures. Minority carrier diffusion is symmetric about the generation point, but blocked along one axis by the presence of the NSOM probe.

Carrier diffusion lengths can be extracted from the intensity variation for a range of sample and excitation geometries, assuming one applies the appropriate model for diffusion. If the surface recombination is small (S~0 cm/s, as in the case of a thin film double heterostructure), then the diffusion equations are relatively straight-forward and are summarized in Figure 8 for a variety of cases. The ability to operate the SEM in a line mode, in addition to spot mode, brings added symmetry to the problem and provides a way to measure submicron spatial variations in thin film and bulk materials from a single image. When surface recombination plays a significant role, then its effect on the diffusion profiles must be included and additional relevant length scales come into play. Examples addressing 1D, 2D and 3D diffusion with finite S are presented in Refs. [34–36].

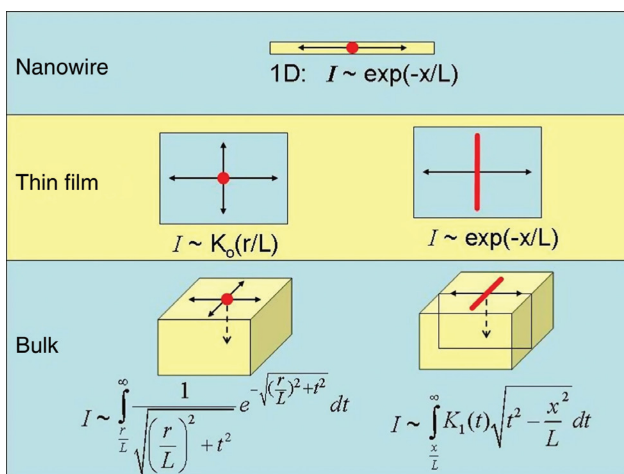

Figure 8 Sample and excitation geometries and corresponding diffusion profiles.

Baird et al. used transport imaging in the SEM to study the diffusion of excess carriers in GaN nanowires, for nanowires with both AlGaN (larger bandgap) and InGaN (smaller bandgap) “shells”, as well as unpassivated surfaces [37]. Figure 9 shows a representative near-field luminescent map, which reflects both carrier diffusion and resulting recombination along the wire, as well as waveguiding of light generated primarily at the spot of excitation to the end of the wire. This image was acquired with a 250 nm collecting probe, with excitation from a 20 keV electron beam, with the beam in spot mode and located at a fixed point on the wire just above the image.

Treating the problem as one-dimensional diffusion from a quasi-point source, estimates of diffusion length for the excess carriers can be extracted from the luminescence profile. However, the clear evidence for a significant

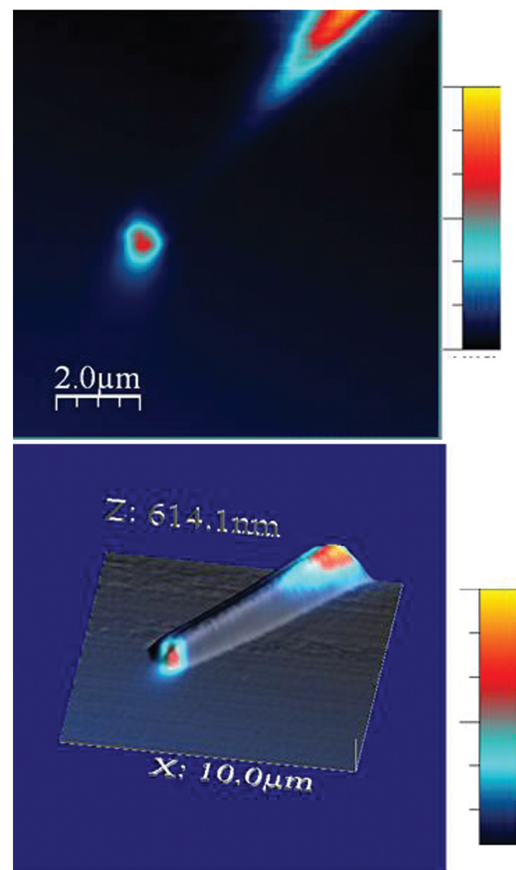

Figure 9 NSOM image of minority carrier diffusion and waveguiding in GaN nanowire. Top image shows NSOM image. Lower image, NSOM signal superimposed on nanowire topography. The color scale shows increasing intensity bottom to top and indicates photon counts in arbitrary units. Adapted from Ref. [37].

Brought to you by | Arthur Lakes Library
Authenticated | 10.248.254.158
Download Date | 8/24/14 1:24 PM

amount of waveguided light that is observed when scanning the collection tip at the end of the wire also makes this a good test case for the detection of the evanescent signal from light that is totally internally reflected at the surfaces. In Figure 10, we have enhanced the contrast along the backbone of the wire to bring out this additional component. Further studies for collection as a function of distance from the surface (ranging from "in contact" to the far-field, with sufficient resolution of the intermediate region) would be of interest to further quantify the contributions.

One important challenge in this configuration is being able to demonstrate that any contribution to the luminescence signal from electron beam interaction with the NSOM tip, whether direct or scattered, is negligible. Glass fibers under electron beam excitation can produce broad visible luminescence associated with defect and other emission. A CL spectrum for common SiO_2 fiber material under 20 keV excitation is shown in Figure 11.

For measuring luminescence associated with transport in a material like GaN, with primary emission in the UV part of the spectrum, filtering can be used to basically eliminate any contribution from luminescence created directly by the electron beam in the probe, as evidenced by the series of scans in Figure 12. These were obtained as the electron beam was fixed at a point on the sample surface (a Si sample without any significant luminescent emission) and the collecting probe was scanned in a raster pattern that placed it initially under the incident electron beam and then scanned away, as occurs in a transport imaging scan. One sees that with a combination of 450 nm and 400 nm short pass filters, this background signal can be eliminated. The problem remains, however, for studies of luminescent materials with very short diffusion lengths and emission

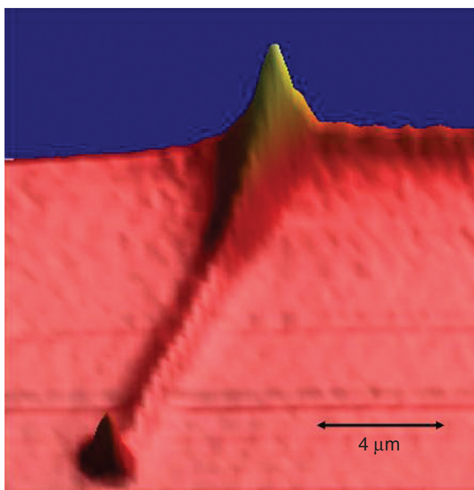

Figure 10 Enhanced constrast NSOM image along a GaN nanowire excited at a single point at the upper edge of the structure.

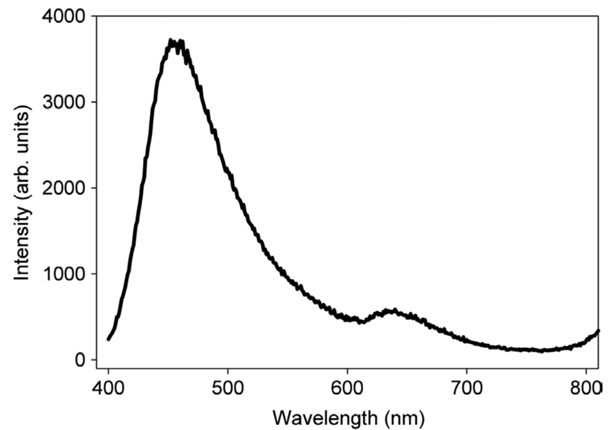

Figure 11 Cathodoluminescence spectrum of SiO_2 fiber under 20 keV excitation.

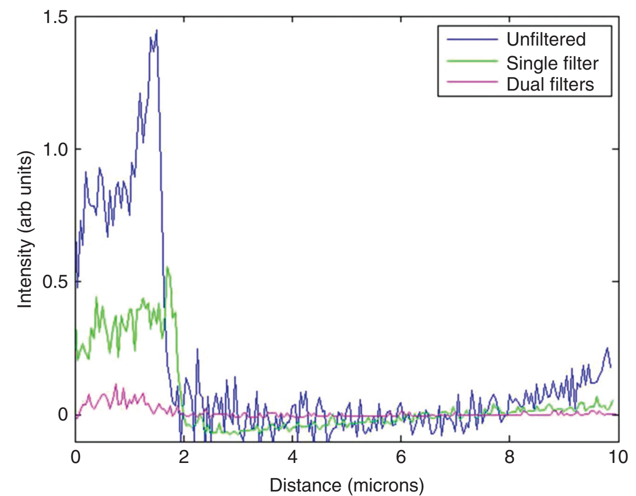

Figure 12 Effect of filtering on optical signal resulting from scanning NSOM probe under direct electron beam excitation. NSOM tip is initially scanned directly under the electron beam and then translated with the slow scan axis in the x direction.

in the range from 400 to 500 nm. In this case, one must demonstrate that the intensity of the luminescence from the material of interest exceeds background signal from the electron beam/tip interaction, especially in determining the slope of the luminescent distribution immediately adjacent to the point of excitation.

Several recent studies have focused on the behavior of effective carrier diffusion length and lifetime in ZnO nanowires as a function of nanowire diameter. Soudi et al. used near-field scanning photocurrent to measure the carrier diffusion length for nanowires with diameters ranging from ~28 to 60 nm [38]. They used near-field illumination probes of aperture size 100–150 nm to locally create carriers which were then collected after diffusing to a reverse-biased Schottky contact. By measuring the photocurrent

Brought to you by | Arthur Lakes Library
Authenticated | 10.248.254.158
Download Date | 8/24/14 1:24 PM

in the absence and presence of above bandgap light illuminating the entire structure, they differentiate between bulk diffusion length and a surface-dependent diffusion length affected by acceptor-type surface states [39].

We have recently performed transport imaging measurements with NSOM in the SEM to measure 300 K carrier diffusion lengths in ZnO nanowires of larger dimensions. Our results are shown in Figure 13, combined with the NSOM photocurrent results and widely ranging reports (as indicated by the far-right vertical line) on bulk or thin film ZnO from electron beam induced current and TRPL measurements [40–42].

For the development of detailed models for transport in smaller structures with real effects from surfaces and materials variations, multiple measurements as a function of the dimensions of the structures will be required. Transport imaging in the SEM can provide this information, because of its ability to easily access and measure multiple structures without the need for contacts. In principle, the whole range of individual structures seen in Figure 6 could be measured on a single substrate and with ease of motion of the electron beam to measure both the physical dimension and the transport properties of interest.

Localized transport of energy can occur optically as well as via carrier diffusion. Figure 14 shows an example of carrier diffusion and waveguided emission from both ends of a GaN nanowire as well as NSOM mapping in a ZnO nanobelt. Integrated electron-beam/NSOM is a useful approach for the study of the optical behavior of nanostructures; the highly localized nature of the excitation allows for measurement of the attenuation coefficient of a single nanowire. The experiment was structured as shown in Figure 15, where the electron beam is placed in spot mode at varying distances from the end of the wire and measurements made of the intensity and distribution of the emitted light that is waveguided down the structure. Emission has been detected for waveguiding at distances up to 60 μm. By measuring the intensity as a function of distance, a Beer's law analysis has been performed, allowing effective attenuation coefficients to be measured as a function of nanowire diameter [43]. This type of approach could be applied to measure localized absorption/transmission across boundaries, defects or interfaces, or within very small structures designed for the local control and transport of light.

Experimental challenges in this form of dual beam transport imaging are similar to those with the near-field

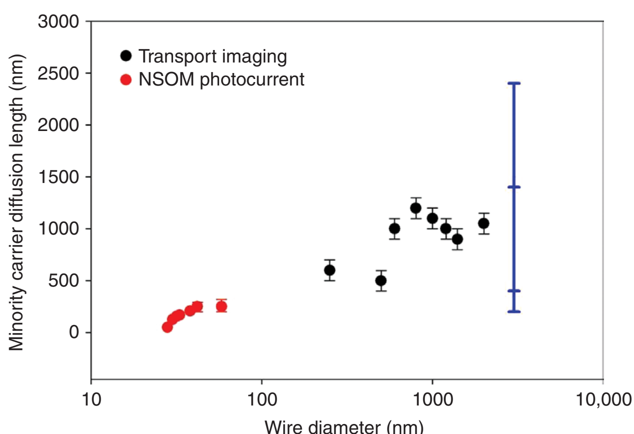

Figure 13 Excess carrier diffusion lengths measured in ZnO nanowires of varying dimensions with NSOM photocurrent and optical transport imaging. All measurements are reported for room temperature.

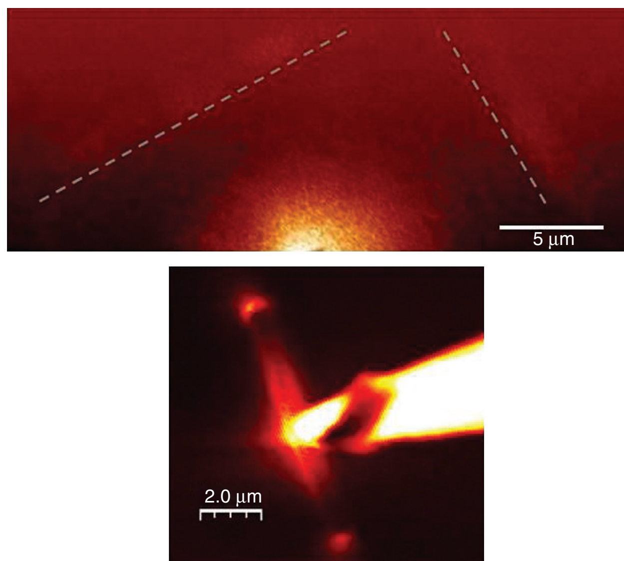

Figure 14 NSOM panchromatic transport imaging of carrier diffusion and waveguiding in ZnO nanobelt (~100 nm thick) (upper) and GaN nanowire (~300 nm diameter) (lower). The dashed grey lines in the nanobelt (upper) figure have been added to aid the eye and mark the physical edge of the nanobelt.

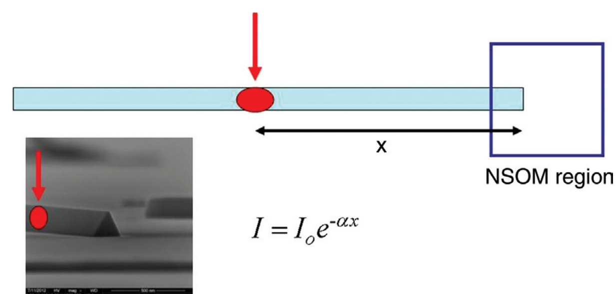

Figure 15 Use of dual probe capability for measurement of absorption coefficient in individual ZnO nanowire. Reprinted from Ref. [43]. The red arrow indicates the point of incidence (spot mode) of the electron beam and x represents the distance from the point of incident to the end of the wire.

Brought to you by | Arthur Lakes Library
Authenticated | 10.248.254.158
Download Date | 8/24/14 1:24 PM

CL: the relatively low throughput for collection through the NSOM probe, topography-related artifacts, limitations on resolution associated with the electron-beam generation volume, and associated trade-offs between luminescent intensity and the electron beam excitation energy. In addition, charging and associated drift of the sample and the NSOM probe must always be addressed, particularly for non-metallic samples. However, we have found that careful grounding for the metal-coated probes, coupled with sample grounding and the use of the lowest possible probe current can significantly minimize these effects.

The integration of a commercially available system, with the capacity for independent scanning of the tip, has been a significant step forward for near-field transport imaging in the SEM. Although diffusion lengths can in principle be estimated by scanning the electron beam with the collecting tip fixed at a point on the sample, as was discussed in [6] and [19], any variation in the generation location does change the nature of the experiment in a non-uniform material. The ability to scan the collecting tip enables the study of transport from a given point. It also allows the type of optical mapping shown in Figures 9 and 14.

Future applications will likely include very high resolution of transport parameter mapping around defects, interfaces and in the interior of increasingly small structures. Modulation of the electron beam will be required to apply lock-in techniques to increase the detection sensitivity so that smaller probe apertures can be used. For structures to which an external bias can be applied, drift of free carriers could be observed, similar to observations of far-field carrier drift using transport imaging in the SEM for thin films [27, 30]. Finally, one can envision a variety of time-resolved measurements that would expand the range of observed phenomena.

5 Future applications and directions

Future applications and directions that integrate electron beam and near-field optics will encompass a wider range of energy-transfer phenomena and likely take significant steps forward as commercial capability advances. Developments to watch include the following:

1. Near-field mapping of electron beam generated near-surface plasmons

The growing field of plasmonics shares two important characteristic behaviors that have been addressed here: the ability to generate light with an electron beam and the ability to transport energy. Electron beams have proven to be an effective means for very high resolution generation of plasmonic resonances [18] and NSOM has played an important role in local excitation and mapping of plasmonic emission [7, 44]. More recently, CL has been used to image the angular distribution of emitted light from planar nanometallic parabolic antennas with subwavelength optical resolution [45] and dual probe NSOM has been applied to visualize nanoscale behavior of propagation of locally excited surface plasmon polaritons [46].

Extremely high resolution CL images can be produced in a scanning transmission microscope, where the very thin nature of the sample limits interaction volume. Figure 16 shows an example of polarized CL images produced in a TEM using 200 keV electrons, with optical collection via an ellipsoidal mirror directing light to an external monochromator [18, 47]. For this type of excitation mapping, the resolution exceeds what can be achieved with NSOM probe collection, given the various practical limitations on the smallest tip apertures. Although experimentally challenging, one could envision near-field collection to enable transport imaging in related structures, which would require a second near-field imaging probe.

Finally, single photon state generation and detection have been very recently demonstrated using 60–100 keV electrons in a scanning transmission electron microscope, utilizing the properties of nitrogen-vacancy (NV) centers in diamond [48]. In addition to the implications for quantum nano-optics, this represents the observation of individual point defects with cathodoluminescence. At the same time, the resolution for studying interaction between neighboring systems remains limited by diffusion, indicating the remaining importance of imaging *transport*, in addition to excitation.

2. Near-field EBIC and device reliability

Other SPM probe systems that have been integrated into scanning electron microscopes have been primarily for electron-beam-induced current measurements. Since resolution of feature sizes of modern electronic devices now requires SEM imaging, techniques that allow for local probing and *in-situ* operation and observation are of growing interest.

Electron-beam-induced current (EBIC) uses an electron beam to create free charge in semiconductors and then measures current collection at a contact to locate p-n junctions, measure carrier diffusion and study surface and recombination effects. Like standard CL, its resolution has been limited by the interaction volume. The use of a small scanning probe to collect the current has been demonstrated to increase the resolution of EBIC

Brought to you by | Arthur Lakes Library
Authenticated | 10.248.254.158
Download Date | 8/24/14 1:24 PM

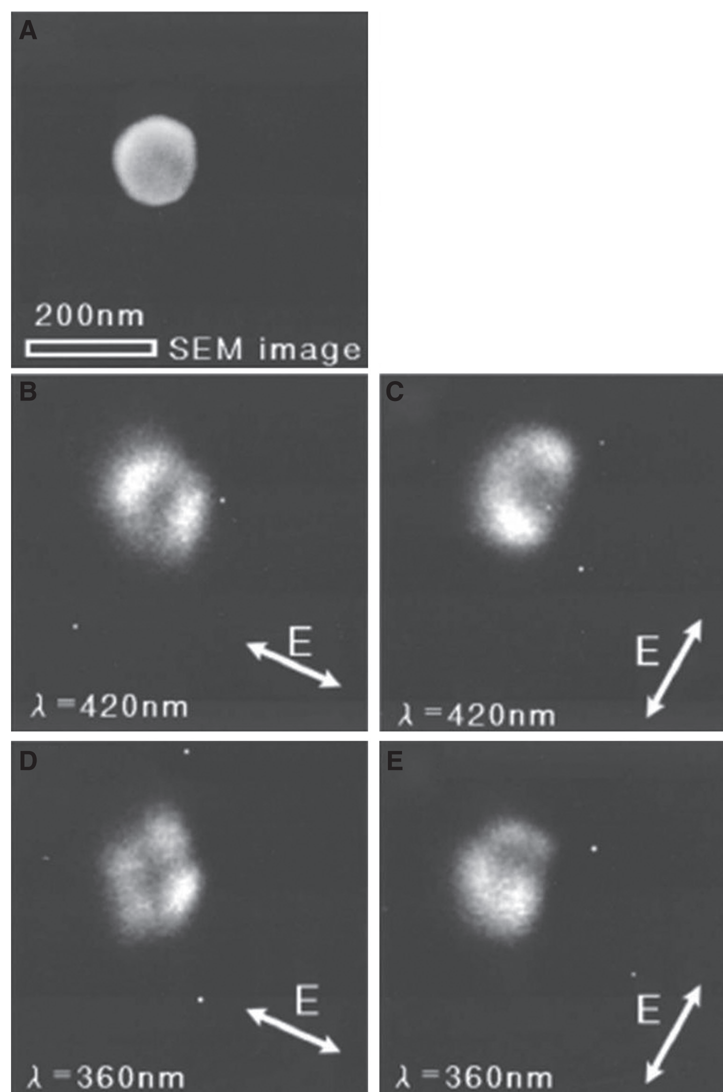

Figure 16 Polarized CL emission from excitation of 140 nm diameter Ag particle. Reprinted Figure 3 from Ref. [47]. Copyright 2001 by the American Physical Society.

[49–51]. The integration of AFM/SPM systems into SEMs will allow for a range of experiments, with variations in the type of scanning probe, that could couple electrical characterization with optical transport imaging, including for devices under bias. With the use of dual probe systems, electrical probes could be used for application of fields or creation of highly localized collecting junctions, followed by optical transport imaging via the NSOM tip for a structure under bias. Not only diffusion but also drift and other types of high field transport could be directly observed.

3. Energy transfer in biological systems

Energy transfer through charge motion observed via distributed luminescence is of interest in a growing number of biological systems. Transport imaging experiments can measure this energy transport since many of the systems of interest can be luminescent in some form [52]. Near-field transport imaging in the SEM would allow for imaging of the structure and the type of dual beam and highly localized transport experiments that are difficult to do with far-field optical excitation, given the relatively small lengths associated with the charge transport. Challenges to be anticipated are low levels of luminescence from very thin structures and damage or bleaching effects associated with the electron beam.

One approach to avoid the damage effects associated with direct interaction in biological samples would be to use remote nanoscale excitation, generated by an electron beam in an adjacent luminescent material. Kaz et al. have demonstrated the generation of nanoscale optical emission in very thin layers of a cerium-doped yttrium

Brought to you by | Arthur Lakes Library
Authenticated | 10.248.254.158
Download Date | 8/24/14 1:24 PM

aluminum perovskite in a Zeiss Gemini Supra 55 scanning electron microscope (Zeiss, Oberkochen, Germany) [53]. They propose utilizing free standing films in contact with biological or soft matter samples to enable a scannable nanoscale optical source for high resolution CL. While challenges will exist to optimize scintillator film thickness, sample thickness and electron excitation energy for high resolution optical coupling while limiting any electron beam interaction, this approach holds promise for effective near-field scanning optical microscopy without the need for mechanical NSOM scanning for biological films.

4. Variable temperature capability and commercial integration of NSOM with SEM

All systems described to date that integrated SEM and NSOM have operated with the sample at room temperature. However, low temperature NSOM has been demonstrated, both for systems with the entire NSOM immersed in liquid helium [14] and for a cold-finger approach where the NSOM scanning system operates in vacuum [54]. This latter approach would be feasible for independent incorporation into SEMs or for development of NSOM systems in SEM with existing cold stages. The interest in nanoscale transport in low temperature systems would justify the complexity and open a range of otherwise inaccessible transport studies.

In 2010, the major SEM manufacturer FEI announced a collaborative agreement with Nanonics Imaging to explore the feasibility of integrating an AFM into an SEM/FIB (focused ion beam) dual beam systems. A prototype demonstration system was described at the 2012 Microscopy and Microanalysis meeting [55]. The scanning probe microscope was integrated with a Dual Beam SEM/FIB system that allowed for imaging of the exposed probe tip with immersion objectives at a working distance as low as 4 mm. The goal is a system in which a variety of probes (NSOM as well as AFM, thermal, magnetic or electrical) could be implemented within a single system framework. Although the initial driving force may be nanometric height profiling to monitor FIB modifications *in-situ*, commercial capability in this regard could lead to increased use and performance of NSOM systems for the study of spatial variations and energy transport.

6 Conclusion

The integration of electron beam, AFM and near-field optical imaging offers exciting capabilities for combining high resolution topography and optical imaging for the nanoworld. Instruments to date have been used for near-field CL, imaging of spatially resolved carrier transport and optical measurements in individual nanowires. The power of electron beams to generate highly localized electronic and optical excitation enables application of this combined capability to studies of semiconductor devices, nano-based laser structures and a wide range of emerging plasmonic structures and devices for integrated nano-optics.

Challenges exist in the areas of throughput, stability of sample and NSOM probes under electron beam excitation and the characterization of complex interactions between the electron beam, the near-field radiation and the scanning probe. However, the potential for unique experiments that provide direct insight into energy transport and nanoscale materials variations and defect structures will drive the development of improved systems. While the electron beam already provides one highly localized and highly versatile probe in a dual probe configuration, future developments will include applications with multi-probe systems to allow application of bias and *in-situ* imaging of transport in operating devices. Growing commercial interest in combining *in-situ* AFM imaging with focused-ion-beam capability is likely to accelerate the growth of the community of users and the range of scientific applications.

Acknowledgements: The following individuals contributed greatly to some of the work described in this manuscript during their time as graduate students or summer interns: Lee Baird, Chun-Hong Low, Abigail Hoffman, Anree Little, Daniel Chisholm, R. Adam Cole, David Phillips and Kevin Blaine. I thank my collaborators, as well as colleagues who have provided samples: Clyde Scandrett, Chris Frenzen, Thomas Boone, Alec Talin, George Wang and Z. L. Wang. Helpful discussions and insights are acknowledged with: Prof. Aaron Lewis, Hesham Taha, Andrey Ignatov and Ben Yacobi. Transport imaging work with combined SEM and NSOM has been supported by the National Science Foundation through Grants DMR-0526330 and DMR 0804527 and through the NSF/DHS ARI program under Interagency Agreement HSHQDC-11-X-0015. N.M.H also acknowledges support for work on this topic as a Fulbright Senior Scholar at Hebrew University in 2012.

Received September 3, 2013; accepted November 5, 2013; previously published online December 6, 2013

Brought to you by | Arthur Lakes Library
Authenticated | 10.248.254.158
Download Date | 8/24/14 1:24 PM

References

[1] Synge EH. A suggested model for extending microscopic resolution into the ultra-microscopic region. Phil Mag 1928;6:356–62.

[2] Dannen G. Leo Szilard the inventor: a slideshow. Copyright Gene Dannon 1998 (available at www.dannen.com/budatalk.html). Posted April 20, 1998, accessed August 15, 2013.

[3] Ash EA, Nicholls G. Super-resolution aperture scanning microscope. Nature 1972;237:510.

[4] Joachimsthaler I, Heiderhoff R, Balk FJ. A universal scanning-probe-microscope-based hybrid system. Meas Sci Technol 2003;14:87–96.

[5] Troyon M, Pastre D, Jouart JP, Beaudoin JL. Scanning near-field cathodoluminescence microscopy. Ultramicroscopy 1998;75:15–21.

[6] Cramer RM, Ebinghaus V, Heiderhoff R, Balk LJ. Near-field detection cathodoluminescence investigations. J Phys D: Appl Phys 1998;31:1918–22.

[7] Dallapiccola R, Dubois C, Gopinath A, Stellacci, Dal Negro L. Near-field excitation and near-field detection of propagating surface plasmons on Au waveguided structures. Appl Phys Lett 2009;94:243118.

[8] Kaneta A, Fujimoto R, HaSimoto T, Mishimura K, Funato M, Kawakami Y. Instrumentation for dual-probe scanning near-field optical microscopy. Rev Sci Instrum 2012;83:083709 and references therein.

[9] Kim JH, Song KB. Recent progress of nano-techology with NSOM. Micron 2007;38:409–26.

[10] Lucas M, Riedo E. Invited review article: combining scanning probe microscoy with optical spectroscopy for applications in biology and materials science. Rev Sci Instrum 2012;83:061101.

[11] Yacobi B, Holt D. Cathodoluminescence microscopy of inorganic solids. New York: Plenum Press; 1990.

[12] Hamann HF, Gallagher A, Nesbitt DJ. Near-field fluorescence imaging by localized field enhancement near a sharp probe tip. Appl Phys Lett 2000;76:1953–5.

[13] Safvi SA, Liu J, Kuech TF. Spatial resolution of localized photoluminescence by near-field scanning optical microscopy. J Appl Phys 1997;82:5352–9.

[14] Grober RD, Harris TD, Trautman JK, Betzig E. Design and implementation of a low temperature nearfield scanning microscope. Rev Sci Instrum 1994;65:626–31.

[15] Pastre D, Troyon M. Scanning near-field cathodoluminescence microscopy for semiconductor investigations: a theoretical study. J Appl Phys 1999;86:4326–32.

[16] Pastre D, Bubendorff JL, Troyon M. Resolution in scanning near-field cathodoluminescence microscopy. J. Vac. Sci. Technol. B 2000;18:1138–43.

[17] Heiderhoff R, Sergeev OV, Liu YY, Phang JCH, Balk LJ. Comparison between standard and near-field cathodoluminescence. J Crystal Growth 2000;210:303–6.

[18] Garcia de Abajo FJ. Optical excitations in electron microscopy. Rev Modern Phys 2010;82:209–75.

[19] Nogales E, Joachinsthaler I, Heiderhoff R, Piqueras J, Balk LF. Near-field cathodoluminescence studies on n-doped gallium nitride films. J Appl Phys 2002;92:976–8.

[20] Bethe HA. Theory of diffraction by small holes. Phys Rev 1944;66:163–82.

[21] Neumann L, Pang Y, Houyou A, Juan ML, Gordon R, van Hulst NF. Extraordinary transmission brightens near-field fiber probe. Nanoletters 2011;11:355–60.

[22] Höpfel RA, Shah J, Wolff PA, Gossard AC. Negative absolute mobility of minority electrons in GaAs quantum-wells. Phys Rev Lett 1986;56:2736–9.

[23] Logue FP, Fewer DT, Hewlett SJ, Jordan C, Donegan JF, McCabe EM, Hegarty J, Taniguchi S, Hino T, Nakano K, Ishibashi A. Optical measurement of the ambipolar diffusion length in a ZnCdSe-ZnSe quantum well. J Appl Phys 1997;81:536–8.

[24] Boone TD, Tsukamoto H, Woodall JM. Intensity and spatial modulation of spontaneous emission in GaAs by field aperture selecting transport. Appl Phys Lett 2003;82:3197–9.

[25] Fickenscher, MA, Jackson HE, Smith LM, Yarrison-Rice JM, Kang JH, Paiman S, Gao Q, Tan HH, Jagadish C. Direct imaging of the spatial diffusion of excitons in single semiconductor nanowires. Appl Phys Lett 2011;99:263110.

[26] Haynes JR, Shockley W. The mobility and life of electrons and holes in germanium. Phys Rev 1951;81:835–43.

[27] Luber DR, Bradley FM, Haegel NM, Talmadge MC, Coleman MP, Boone TD. Imaging transport for the determination of minority carrier diffusion length. Appl Phys Lett 2006;88:163509.

[28] Haegel NM, Mills TJ, Talmadge M, Scandrett C, Frenzen CL, Yoon H, Fetzer CM, King RR. Direct imaging of anisotropic minority-carrier diffusion in GaInP. J Appl Phys 2009;105:023711.

[29] Haegel NM, Williams SE, Frenzen CL, Scandrett C. Minority Carrier Lifetime Variations Associated with Misfit Dislocation Networks in Heteroepitaxial GaInP. Semicon Sci Tech 2010;25:055017.

[30] Andrikopoulus P, Boone TD, Haegel NM. Localized electric field mapping in planar semiconductor structures. IEEE Trans Electron Dev 2008;55:1529–34.

[31] Phillips D, Blaine K, Haegel NM, Campo G, Cirigno L. Cathodoluminescence and spatial variation in the mobility-lifetime product in thallium bromide. IEEE Trans Nucl Sci 2012;59:2608–13.

[32] Haegel NM, Low CH, Baird L, Ang GL. Transport imaging with near-field scanning optical microscopy. Proc. SPIE 7378, Scanning Microscopy 2009, 73782B (May 22, 2009).

[33] Haegel NM, Chisholm DJ, Cole RA. Imaging transport in nanowires using near-field detection of light. J Crystal Growth 2012;352:218–23.

[34] Allen JE, Hemesath ER, Perea DE, Lensch-Falk JL, Li ZY, Yin F, Gass MH, Wang P, Bleloch AL, Palmer RE, Lauhon LJ. High-resolution detection of Au catalyst atoms in Si nanowires. Nat Nanotechnol 2008;3:168–73.

[35] van Roosbroeck W. Injected current carrier transport in a semi-infinite semiconductor and the determination of lifetimes and surface recombination velocities. J Appl Phys 1955;26:380–91.

[36] Blaine KE, Phillips DJ, Frenzen C, Scandrett C, Haegel NM. Three dimensional transport imaging for the spatially resolved determination of carrier diffusion length in bulk materials. Rev Sci Instrum 2012;83:043702.

[37] Baird L, Ong CP, Cole RA, Haegel NM, Talin AA, Li Q, Wang GT. Transport imaging for contact-free measurements of minority

Brought to you by | Arthur Lakes Library
Authenticated | 10.248.254.158
Download Date | 8/24/14 1:24 PM

carrier diffusion in GaN, GaN/AlGaN and GaN/InGaN core-shell nanowires. Appl Phys Lett 2011;98:132104.
[38] Soudi A, Dhakal P, Gu Y. Diameter dependence of the minority carrier diffusion length in individual ZnO nanowires. Appl Phys Lett 2010;96:253115.
[39] Soudi A, Hsu CH, Gu Y Diameter-dependent surface photovoltage and surface state density in single semiconductor nanowires. Nanoletters 2012;12:5111–6.
[40] Lopatiuk O, Chernyak L, Isinsky A, Xie JQ, Chow PP. Eelctron-beam-induced current and cathodoluminescence studies of thermally activated increase for carrier diffusion length and lifetime in n-type ZnO. Appl Phys Lett 2005;87:162103.
[41] Lopatiuk-Tirpak O, Chernyak L. Studies of minority carrier transport in ZnO. Superlattices Microst 2007;42:201–5.
[42] Koida T, Chichibu SF, Uedono A, Tsukazaki A, Kawasaki M, Sota T, Segawa Y, Koinuma H. Correlation between the photoluminescence lifetime and defect density in bulk and epitaxial ZnO. Appl Phys Lett 2003;82:532.
[43] Little A, Hoffman A, Haegel NM. Optical attenuation coefficient in individual ZnO nanowires Opt Express 2013;21:6321–6.
[44] Maier SA, Kik PG, Atwater HA, Meltzer S, Harel E, Koel BE, Requicha AAG. Local detection of electromagnetic energy transport below the diffraction limit in metal nanoparticle plasmon waveguides. Nat Mater 2003;2:229–32.
[45] Schoen DT, Coenen T, Garcia de Abajo FJ, Brongersma ML, Polman A. The planar parabolic optical antenna. Nanoletters 2013;13:188–93.
[46] Fujimoto R, Kaneta A, Okamoto K, Funato M, Kawakami Y. Interference of the surface plasmon polaritons with an Ag waveguide probe by dual-probe scanning near-field optical microscopy. Appl Surface Sci 2012;258:7372–6.
[47] Yamamoto N, Araya K, Garcia de Abajo FJ. Photon emission from silver particles induced by a high-energy electron beam. Phys Rev B 2001;64:205419.
[48] Tizei LGH, Kociak M. Spatially resolved quantum nano-optics of single photons using an electron microscope. Phys Rev Lett 2013;110:153604.
[49] Heiderhoff R, Cramer RM, Balk LJ. IEEE International Reliability Physics Proceedings, 34th Annual IEEE, 96CH35825, 366 1996.
[50] Troyon M, Smaali K. Scanning near-field electron beam induced current microscopy: application to III-V heterostructures and quantum dots. Appl Phys Lett 2007;90:212110.
[51] Smaali K, Faure J, El Hdiy A, Troyon M. High-resolution scanning near-field EBIC microscopy: application to the characterization of a shallow ion implanted p+-n silicon junction. Ultramicroscopy 2008;108:605–12.
[52] Escalante M, Lenferink A, Zhao Y, Tas N, Huskens J, Hunter CN, Subramanium V, Otto C. Long-range energy propagation in nanometer arrays of light harvesting antenna complexes. Nanoletters 2010;10:1450–7.
[53] Kaz DM, Bischak CG, Hetherington CL, Howard HH, Marti X, Clarkson JD, Adamo C, Schlom DG, Ramesh R, Aloni S, Ogletree FD, Ginsberg NS. Bright cathodoluminescent thin films for scanning nano-optical excitation and imaging. ACS Nano 2013;7:10397–404.
[54] Behme G, Richter A, Süptitz B, Lienau CH. Vacuum near-field scanning optical microscope for variable cryogenic temperatures. Rev Sci Instrum 1997;68:3458–63.
[55] Ignatov A, Komissar A, Geurts R. On-line scanned probe microscopy transparently integrated with dual beam SEM/FIB systems. Microsc Microanal 2012;18/S2:640–1.

Brought to you by | Arthur Lakes Library
Authenticated | 10.248.254.158
Download Date | 8/24/14 1:24 PM